University of Tehran Press

Journal of the Earth and Space Physics

Homepage: https://jesphys.ut.ac.ir

Vol. 48, No. 4, Winter 2023, P. 173-182
(Research Article)

Spatial Analysis of $PM_{2.5}$ Concentration over Iraq during 2003-2020

Sadar, M. W.[1] | Al-Jiboori, H. M.[2] ✉ | Al-Timimi, K. Y.[3]

1. Department of Atmospheric Sciences, College of Science, Mustansiriyah University, Baghdad, Iraq. E-mail: wid9777@yahoo.com
2. **Corresponding Author**, Department of Atmospheric Sciences, College of Science, Mustansiriyah University, Baghdad, Iraq. E-mail: mhaljiboori@gmail.com
3. Department of Atmospheric Sciences, College of Science, Mustansiriyah University, Baghdad, Iraq. E-mail: yaseen.k.abbas@gmail.com

(Received: 21 June 2022, Revised: 16 July 2022, Accepted: 4 Oct 2022, Published online: 5 March 2023)

Abstract

The particulate matter with a diameter of 2.5 µm ($PM_{2.5}$) concentration seriously impacts the environment, climate, and human health. $PM_{2.5}$ emissions are caused by anthropogenic or natural sources and are still a problem worldwide. In this study, monthly, seasonal, and annual spatial distributions of $PM_{2.5}$ concentrations were analyzed over Iraq for the period 2003 to 2020 by use of the geographic information system technique. The results indicated that the $PM_{2.5}$ concentration was higher in summer than in winter and autumn. The monthly mean maximum values of $PM_{2.5}$ occurred during June and July with 8.4 and 8.7 µg/m^3 over central and southern regions of Iraq, respectively, while monthly means of minimum values were observed during November over northern and western regions. These results conclude that the magnitude of outdoor $PM_{2.5}$ concentrations varies among seasons and regions. Also, the annual means of $PM_{2.5}$ were less than the standard maximum permissible limits, and their seasonal means were smaller than this limit at all seasons.

Keywords: $PM_{2.5}$, Spatial-temporal analysis, Inverse distance weighting, Statistical analysis, Iraq.

1. Introduction

Clean air is an essential prerequisite for human well-being and health (World Health Organization, 2006). Airborne particulate matter pollution is a critical environmental risk factor linked to their potential effects in causing health problems, visibility impairment, and increased mortality and morbidity in humans (Thurston et al., 2016). $PM_{2.5}$ is particulate matter with an equivalent diameter less than or equal to 2.5 µm in aerodynamics (Li et al., 2019). It is the most common source of air pollution and the primary cause of no communicable diseases in the world (Gakidou et al., 2017). Particulate matter in the atmosphere is made up of liquid and solid particles. They are emitted directly from various natural and human processes, including forest fires, agricultural practices, construction projects, and fuel burning, or generated in the air by gases resulting from fuel combustion. They can contain heavy metals, acids, biological and other organic and inorganic materials (Wark & Warner, 1981). The impacts of $PM_{2.5}$ concentrations in the human health sector can be divided into indirect and direct effects. Indirect effects commonly affect a much wider geographic area and are more difficult to control. One of the most dangerous effects is the acidification of freshwater sources. Through oxidation reactions, aerosols such as sulfur and nitrogen oxides are converted into acidic substances such as sulfuric and nitric acid, negatively impacting the fish population and forest ecosystem health (Welburn, 1988). Direct effects such as premature death and cardiovascular and lung disease are caused mainly by exposure to particulate matter (Pope III et al., 2011). PM_{10} and $PM_{2.5}$, respectively, are of special importance as they can reach the upper and lower portions of the respiratory tract of exposed individuals and cause cardiovascular and respiratory illness (Kampa & Castanas, 2008; Thurston et al., 2016). The size of particles is also directly linked to environmental effects like environmental damage and materials damage (Zubkova, 2003).

Several previous studies have analyzed

Cite this article: Sadar, M. W., Al-Jiboori, H. M., & Al-Timimi, K. Y. (2023). Spatial Analysis of $PM_{2.5}$ Concentration over Iraq during 2003-2020. *Journal of the Earth and Space Physics*, 48(4), 173-182. DOI: http//doi.org/10.22059/jesphys.2022.344671.1007441

Publisher: University of Tehran Press.
DOI: http//doi.org/10.22059/jesphys.2022.344671.1007441

Print ISSN: 2538-371X
Online ISSN: 2538-3906

temporally and spatially $PM_{2,5}$ concentrations. For example, Gorai et al. (2018) analyzed the spatio-temporal variance of $PM_{2.5}$ in Delhi, India. Daily $PM_{2.5}$ concentrations were used from November 2016 to October 2017 in different locations distributed in their study's region. They found maximum and minimum spatial variances were observed March and September, respectively (Gorai et al., 2018). Also, Wang et al. (2019) studied the characteristics of the temporal and spatial distributions of particulate matter ($PM_{2.5}$) in Changchun, China, by using hourly particulate matter mass concentration measured at 10 weather automatic monitoring stations. Their results indicated that the quarterly average $PM_{2.5}$ mass concentrations in Changchun were higher in the first quarter, and the fourth quarter was concentrated mainly in the central, northern, and western areas of Changchun (Wang et al., 2019). Finally, Kiai et al. (2021) studied the spatial extent and distribution of $PM_{2.5}$ in Nairobi, Kenya, for seven sites based on the land use type. The highest 24-hour average concentration of $PM_{2.5}$ was observed in Viwandani, an industrial area (111.87 $\mu g/m^3$), and the lowest concentration was found at Karura (21.25 $\mu g/m^3$), a forested area (Kiai et al., 2021).

In previous studies, most scientists analyzed the spatio-temporal rates of $PM_{2.5}$ particles in certain areas. The present study aims to analyze the spatial concentrations of PM2.5 in Iraq from 2003 to 2020, including the means of $PM_{2.5}$ concentration (i.e., monthly, seasonally, and annually) and determining the maximum, minimum, median, average, and standard deviation for concentration $PM_{2.5}$. The data for $PM_{2.5}$ obtained were initially monthly measurements and then analyzed as monthly, seasonal, and annual means for 18 years over all provinces of Iraq. In this study, the spatial analysis for $PM_{2.5}$ concentrations was studied using a geographic Information System (GIS).

2. Study area and data source

The research region is Iraq, which is geographically located in the Northern Hemisphere between latitudes of 29.5° and 37.5°N and longitudes of 38.45° and 48.45°E. Iraq is also located in the southwest corner of the Asian continent, in the northern portion of the Arab Homeland, with Turkey, Syria, and Jordan to the west, Kuwait and Saudi Arabia to the south, and Iran to the east (see Figure 1, left side). The proximity or distance of Iraq from water bodies significantly impacts Iraq's climate and thermal qualities, with the Mediterranean Sea and the Persian Gulf being the most influential water bodies in Iraq (Jassim & Goff, 2006). The topography of Iraq's surface is divided into four main parts in terms of terrain forms to the following areas: the mountains region, which represents the northern and the northeast areas of Iraq with an estimated area of about 5% of the total area of Iraq; plateaus and hills region, located in the south of the mountains regions with an estimated area of about 15%; the plain sedimentary region, which extends from central Iraq to the top of the Persian Gulf, with an estimated area of about 20%; and the western plateau, is the part of the Arabian Peninsula plateau, which extends to broad areas to the south and southeast of the country, with an estimated area of about 60% (Jassim & Goff, 2006).

One of the most significant features of Iraq is the extremely high temperature change in one day (i.e., day and night) and between the summer and winter seasons. Winter is cold, and the temperature ranges from about 2 °C at night and increases to 16 °C in the daytime. Summer is very dry and hot to extremely hot, with the mean temperature in shadow reaching more than 43 °C in July and August, decreasing to 26 °C at night. More feature of Iraq's climate is drought, which occurred because of the shortage of precipitation and its water sources limitations. In addition, the increase of evaporation due to the high quantities of solar radiation residence on the surface causes the increase in the drought (Frenken, 2009). Iraq lies within the moderate northern region, a system similar to the Mediterranean where rainfall occurs almost in winter, sometimes in spring, slightly in autumn, and disappears in summer. The region is often divided into three rainfall zones according to the annual rainfall amounts: northern, middle and southern regions. Rainfall in Iraq varies during the year, approximately from 50 mm in the southwest to 1000 mm in the northeast

(AL-Timimi, 2014). The north and northeast of Iraq usually receive higher amounts of rain than the south.

The ubiquitous nature of atmospheric aerosol shows an intense impact on the earth's atmospheric system, climatic conditions, atmospheric chemistry, influence of weather conditions, ecosystem, air quality and public health (Pöschl, 2005). Moreover, these particles play a critical role in driving climate change because they scatter and absorb solar radiation (Ding et al., 2016; (Fu et al., 2017). Aerosol particles are efficient in absorbing and scattering solar radiation, changing the intensity and direction of sunlight, resulting in a reduction in the atmospheric horizontal visibility (Barber, 1984; Husar et al., 2000). Besides, there are also correlations between $PM_{2.5}$ and some meteorological variables like temperature and wind with which there are a positive correlation, and the wind speed is the most closely associated factor with $PM_{2.5}$. There is a negative correlation with atmospheric pressure and rain, there are positive correlations in some areas and negative correlations in others, and the rain played an important role in reducing pollutant concentrations (Wid et al., 2022).

The monthly data of $PM_{2.5}$ has been acquired from the Copernicus website (https://ads.atmosphere.copernicus.eu/cdsapp#!/search?type=dataset). Copernicus is the European Union's Earth observation program. It offers information services taken from satellite Earth Observation and in-situ (non-space) data**.** The European Commission manages the program for 2003-2020 $PM_{2.5}$ data with unit of $\mu g/m^3$. The horizontal coverage of the global resolution is 0.75°×0.75°, and the total grids are 210, covering the study area and neighborhood as shown on the right side of Figure 1. All grid points in this figure are interpolated to get the final maps of the concentration.

3. Methodology

The spatial distribution of the particle $PM_{2.5}$ is carried out using GIS, which is a computer-based information system that provides tools for the collection, integration, management, analysis, modeling and presentation of data referred to in the accurate graphical representation of objects in space (Hassan, 2018). Many GIS software packages are available, from commercial packages to free and open-source software.

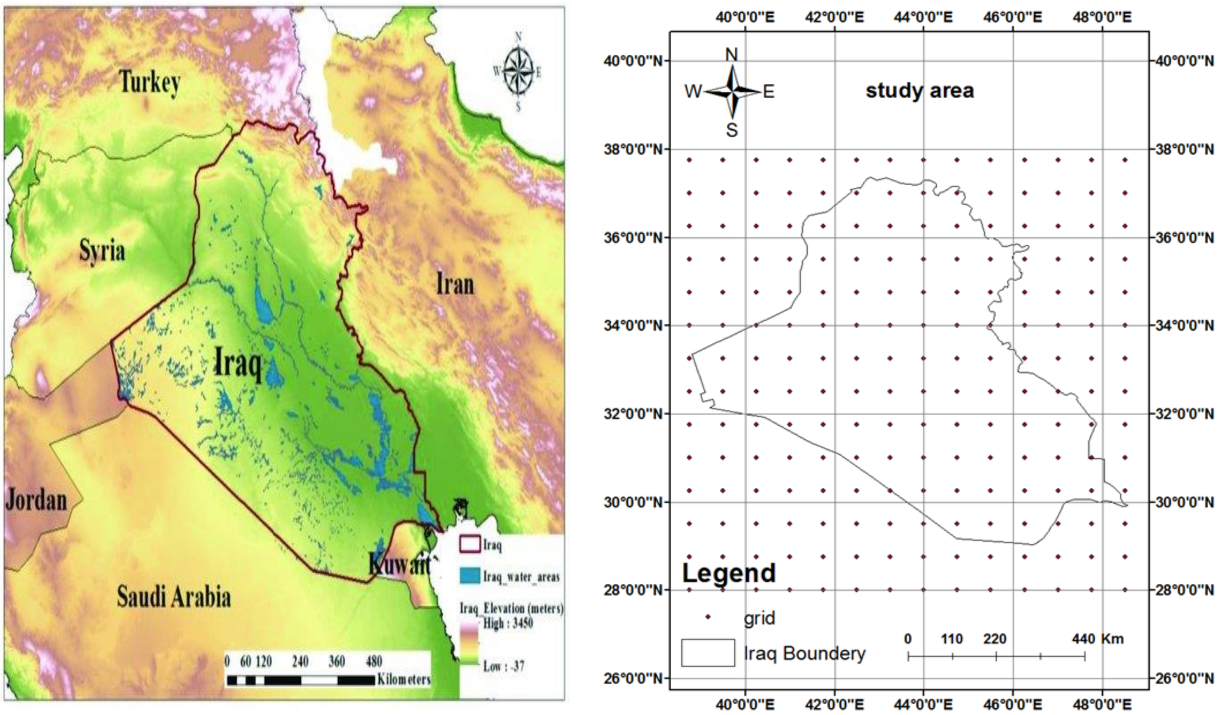

(a) (b)

Figure 1. a) elevation map of Iraq and neighboring countries. b) grid points of the study area of Iraq.

Currently, ArcGIS is probably the most widely used program, developed by the Environmental Systems Research Institute, offering a user-friendly graphic interface, the ability to handle different types of geographic objects, and a set of powerful tools and extensions (Sánka, 2015). Spatial interpolation methods are the estimation of property values in unknown points within a region covered by existing observational points. The spatial interpolation operations in numerous situations are executed in GIS. There are many different approaches to classifying the spatial interpolation procedures, like point interpolation and region interpolation, global and local, and exact and approximate interpolation. Numerous systems exist for both interpolations of local and global, the examples for the global systems are the trend surface analysis and Fourier series, and an example for local technologies are proximal, Kriging, B-splines technique (Huang et al., 2011), and Inverse Distance Weighting (IDW): the practice of using known data to estimate unknown data values. In this interpolation technique, interpolational estimates are based on values from nearby locations that are only weighted by the distance from the interpolation site. Except for the basic assumption that the proximal points in the interpolation site must be more relevant than the far-off points, IDW makes no assumptions about spatial relationships. This method uses a linearly weighted set of sample points to determine cell values. The opposing distance determines the weight. Based on their distance from the output point, IDW allows the user to control the importance of known points on the defined values (Hessl et al., 2007). IDW relies primarily on two assumptions: the first is that the anonymous value of a point is affected by the proximity control points more than the remote points. The degree of impact (weight) of the points corresponds to each other directly, with the inverse distance between the points raised to the force (Huang et al., 2011). IDW needs to have some parameters of the trigger, such as the parameters of the search neighborhood, the exponential factor, and the homogenization factor. It is particularly suitable for limited data sets, where other installation techniques may be affected by errors. This technique is very flexible and allows the evaluation of the data set with the direction or contrast of information in the research area (Garnero & Godone, 2013). In general, the simplified formula for IDW is:

$$V_0 = \frac{\sum_{i=1}^{n}\left[\frac{V_i}{D_i}\right]}{\sum_{i=1}^{n}\left[\frac{1}{D_i}\right]} \tag{1}$$

where V_0 is the predictable value at point 0, V_i is the V value at control point i, D_i is the distance between control point i and 0, and n is the number of known values used in the evaluation (Bajjali, 2017). This weighting relationship affects the giving of data points close to the interpolation point with relatively large weights, while the effect is negligible on distant points (Robinson & Metternicht, 2003).

The arithmetic mean of $PM_{2.5}$ was calculated by Equation (2) (Reimann et al., 2011):

$$\overline{PM_{2.5}}=\frac{1}{n}\sum_{i=1}^{n}(PM_{2.5})_i \tag{2}$$

The counter n indicates the total number of points in the study area, and $(\bar{\ })$ denotes mean. The median divides the data distribution into two halves. The data are sorted from the lowest to the highest value, and the central value of the ordered data is the median. In the case of n being an even number, two central values exist, and the average of these two values is taken as the median (Reimann et al., 2011).

The standard deviation (SD) that describes the average spread of the data around the central value can be calculated by Equation (3) (Reimann et al., 2011):

$$\text{SD}=\sqrt{\frac{1}{n-1}\sum_{i=1}^{n}(PM_{2.5_i}-\overline{PM_{2.5}})^2} \tag{3}$$

4. Results and discussion

4-1. Monthly spatial distribution of $PM_{2.5}$ concentrations

The descriptive statistics of monthly $PM_{2.5}$ concentrations such as mean, SD, maximum and minimum are displayed in Table 1. It can be seen that the monthly ranges of means, SD, maximum, and minimum for the study area (4.6-8.7), (1.8-3.6), (8.5-1.6), and (1-1.9) µg/m^3, respectively.

Table 1. Statistics values of monthly $PM_{2.5}$ concentration included mean, SD, Maximum and Minimum values.

Statistical parameters ($\mu g/m^3$)	**Jan**	**Feb.**	**Mar.**	**Apr.**	**May**	**Jun.**	**Jul.**	**Aug.**	**Sep.**	**Oct.**	**Nov.**	**Dec.**
Mean	5.3	5.7	6	5.2	6.6	8.4	8.7	6.3	5.4	5.5	4.6	5.1
SD	2.1	2.3	2.3	2.4	2.2	3.3	3.6	2.4	2	1.9	1.8	2.1
Maximum	10.5	11.3	10.9	11.5	10.9	16	15	11.1	9.7	9.3	8.5	9.9
Minimum	1.3	1.7	1.8	1.9	1.8	1.6	1.6	1.3	1.1	1.5	1	1.1

Table 1 shows that in the summer months, $PM_{2.5}$ means are higher than the rest of the months, especially in June and July [8.4 ± 3.3] and [8.7 ± 3.6]. The reason for this is due to the arid condition in the summer, the lack of rain, and high solar heating, which leads to the fragmentation of the soil in addition to the instability. We notice lower means in the winter months.

Spatial maps of the monthly averages of $PM_{2.5}$ concentrations over Iraq are displayed in Figure 2. The results show that all maps of monthly distribution of $PM_{2.5}$ concentrations can be divided into fifteen classes of $PM_{2.5}$ concentrations ranging from 1 to 15 $\mu g/m^3$. In the southern side of Iraq, the results of all monthly maps reveal that the $PM_{2.5}$ concentrations are higher than the other parts of the country.

During the summer months, most areas of Iraq witness the presence of high concentrations. The highest values are concentrated in two regions: the southern region and the country's central region. Iraq's highest values are observed during June and July months is 15 $\mu g/m^3$. As shown in Figure 2, the monthly average of $PM_{2.5}$ in the northern and western regions of Iraq does not show severe changes in the values of $PM_{2.5}$ concentrations. Thus, these areas are characterized by having the lowest concentrations of pollutants. The lowest values of $PM_{2.5}$ in these regions is 1 $\mu g/m^3$ during December.

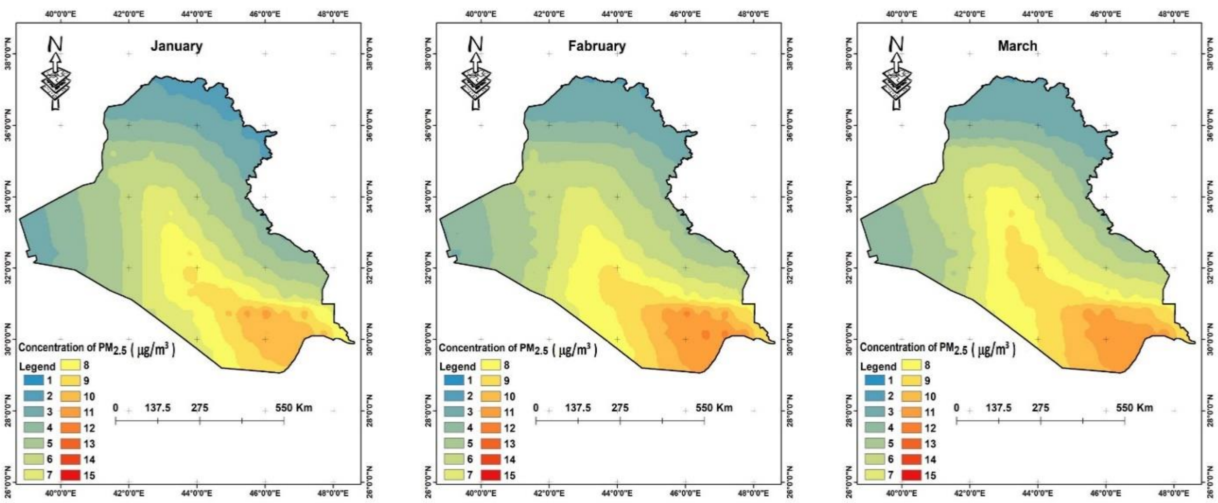

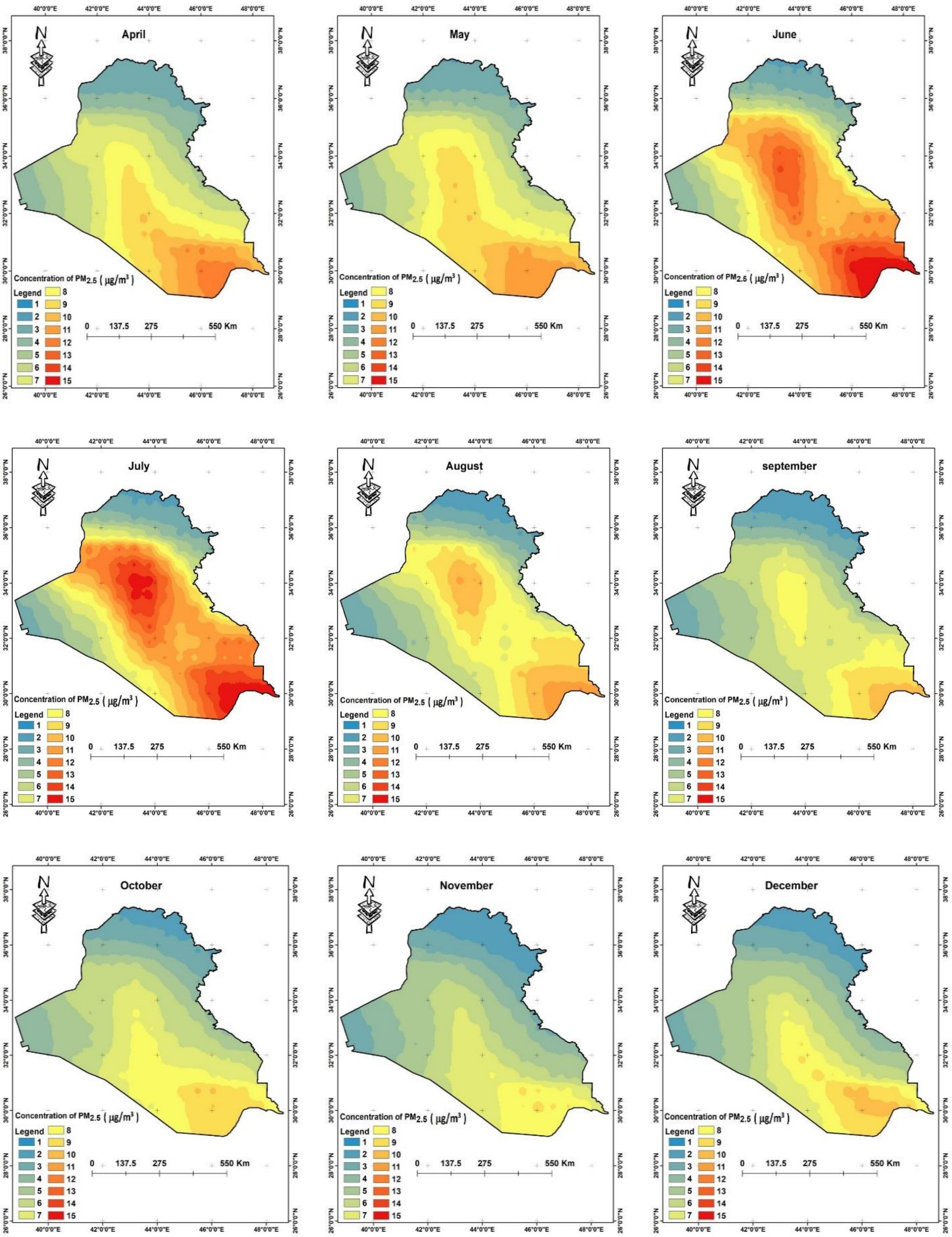

Figure 2. The spatial distributions of monthly $PM_{2.5}$ concentrations over Iraq during 2003-2020.

Figure 3 shows monthly variation in $PM_{2.5}$ concentrations over Iraq during the period of study. The values in the graph present the average and the associated standard deviation (by error bars) for the period 2003–2020. The monthly changes in the standard deviation of

$PM_{2.5}$ are common during all months, except for the highest values in June and July. The most noticeable feature is that the $PM_{2.5}$ concentration reaches its maximum peak in June (8.4 µg/m^3) and July (8.7 µg/m^3) in the study area. This is expected because there is no rain in summer (Al-Timimi, 2012). The $PM_{2.5}$ concentrations begin to increase during January (5.3 µg/m^3), February (5.7 µg/m^3) and March (6 µg/m^3), then decrease during April (5.4 µg/m^3) because of frequent thunderclouds in this month, and then increase again during May (6.6 µg/m^3), June (8.4 µg/m^3) and July (8.7 µg/m^3), reaching their highest value in June. After that, the concentration values begin to decrease from August (6.3 µg/m^3) to November (4.6 µg/m^3), and finally, the values start to increase during December (5.1 µg/m^3).

4-2. Seasonal spatial distribution of $PM_{2.5}$ concentrations

Figure 4 shows the seasonal spatial averages for $PM_{2.5}$ concentration for winter, spring, summer and autumn for the period 2003-2020. During the winter, it can be seen that the maximum concentration, 10 µg/m^3, is found in the south part of Iraq (Basrah and Muthana), while the minimum value of $PM_{2.5}$ concentration is in the north and western regions of Al-Anbar governorate in Iraq. In winter, the seasonal average $PM_{2.5}$ concentration across all regions of Iraq is 5µg/m^3. The behavior of $PM_{2.5}$ concentrations during the spring is similar to the behavior of winter. The average $PM_{2.5}$ concentrations for the spring is 6 µg/m^3. It can be seen that the average of $PM_{2.5}$ concentration started to be higher than that of the winter season. A significant rising in $PM_{2.5}$ concentrations can be observed 7.1µg/m^3 over the middle and southern regions in Iraq during the summer. Meanwhile, during the autumn, the average value of $PM_{2.5}$ concentrations over all regions is decreased to 5µg/m^3.

From the previous figures, it can be noted that the spatial distribution of $PM_{2.5}$ concentration is almost identified in the south regions where the average concentration is higher compared to the northern regions. This means a decline in concentration from south to north. The reason may be due to the human and natural causes that include some climate parameters related to pollutants, namely rainfall and temperature. The northern regions of Iraq receive more amounts of rain compared to the southern regions, and the rain has an inverse relationship with pollutants. Also, the temperatures differ between the north and the south, as the temperatures in the southern regions are higher than the northern regions. The higher concentrations of pollutants are directly proportional to higher temperatures and human sources in the southern regions, where there is a high population, meaning more human activities and more pollution, as the numbers of cars are large in various capacities to emit toxic gases and in huge quantities without the presence of a green belt that can reduce the damages of these toxic gases. The citizens daily burn waste to get rid of it and in large quantities that represents a problem requiring a serious decision to establish waste recycling plants. Which guarantee its transformation into useful materials. In addition to the thousands of scattered private generators, the toxic gases that are emitted from power stations and can be originated from internal sources such as tobacco smoking, cooking and the use of stoves. In addition, it can be from natural sources, such as pollen, dust, etc.

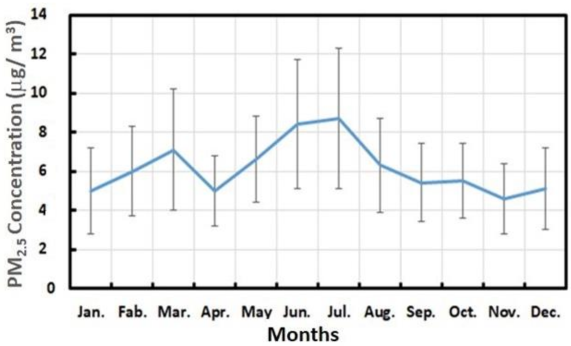

Figure 3. The means of $PM_{2.5}$ concentrations for all months of the year with error bars represent the standard deviation.

In general view, the seasonal spatial distribution of $PM_{2.5}$ has low concentration values in the northern and western regions of Iraq, compared to the southern and southeastern regions. Table 2 shows some statistics for each season of the year such as the total means and their SD, maximum and minimum of $PM_{2.5}$ concentrations, which shows that the concentrations of pollutants rise in the summer and reach [7.1 ±3.1] and decrease in the rest of the seasons; the annual average of concentrations is 6 μg/m^3.

In order to illustrate the level of ambient air pollution with $PM_{2.5}$ concentrations over Iraq, these means are compared to the standard maximum permissible limits, which are widely used as a reference tools by policymakers in the world to set standards and goals for air quality management. This limit states that annual average concentrations of $PM_{2.5}$ should not exceed 10 μg/m^3 (Al-Jiboori, 2015). From seasonal and annual means reported in Table 2, all of them are less than the standard limit, which experience low levels of outdoor air pollution over the year in Iraq.

Table 2. Statistics of the values for seasonal $PM_{2.5}$ concentrations including: mean, SD, maximum and minimum.

Statistical parameters (μg/m^3)	Winter	Spring	Summer	Autumn	Annual
Mean	5	6	7.1	5	6
SD	2.2	2.3	3.1	1.8	2.3
Maximum	10.2	11	14.7	8.5	11
Minimum	1.3	1.7	1.1	1.1	1.5

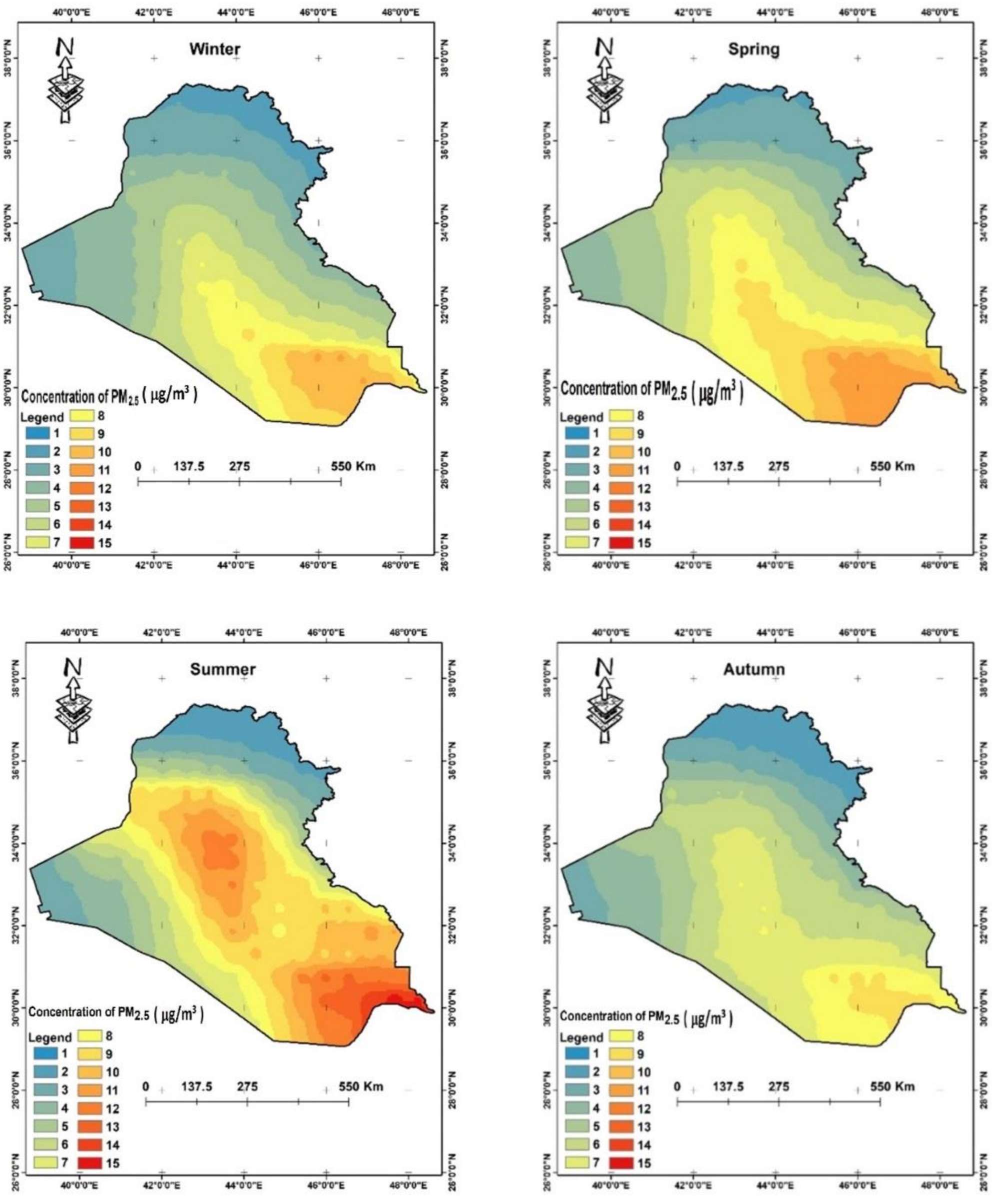

Figure 4. Spatial distribution of the seasonal $PM_{2.5}$ concentrations over Iraq during 2003-2020.

4-3. Annual spatial distribution of $PM_{2.5}$ concentrations

Figure 5 illustrates the annual mean distribution of $PM_{2.5}$ concentrations form 2003 to 2020. The maximum concentrations of $PM_{2.5}$ 11 µg/m^3 just south of Iraq occur on the Iraqi-Kuwait border, characterized by the presence of oil fields and exceed to the maximum permissible limit (10 µg/m^3) over the year (Al-Jiboori, 2015).

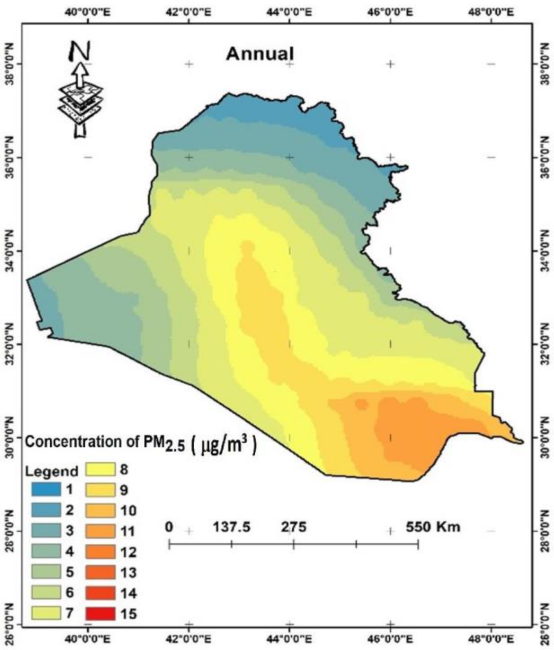

Figure 5. The annual mean of $PM_{2.5}$ concentrations over Iraq during 2003-2020.

5. Conclusions

In this study, the monthly, seasonal and annual distribution of $PM_{2.5}$ concentrations are determined using GIS for 18 years (2003-2020). The monthly $PM_{2.5}$ concentrations reach its highest value in July over southern region, while the lowest value of $PM_{2.5}$ concentrations is in December over the northern region of Iraq. The result shows that the trend of mean $PM_{2.5}$ for annual series has increased over the Iraq for the study period.

The seasonal distribution for $PM_{2.5}$ concentrations shows the fluctuation of highest concentration in the same region during the summer, autumn and spring. The result shows that the highest concentrations of $PM_{2.5}$ are in the south and the middle and is gradually decreasing toward the north region.

Acknowledgments

The authors of the present work express their deepest appreciation to Mustansiriyah University (www.uomustansiriyah.edu.iq) for their support during the work.

References

Al-Timimi, Y. (2012). Assessment of drought in Iraq using standardized precipitation index (SPI) and satellite data. *PhD thesis*, Al-Mustansiriya University.

Al-Timimi, Y.K. (2014). Drought assessment in Iraq using analysis of Standardized precipitation index (SPI). *Iraqi Journal of Physics*, 12(23), 36-43.

Al-Jiboori, M.H. (2015). *Atmospheric Pollution*. Simea Press, p. 219.

Barber, P.W. (1984). Absorption and scattering of light by small particles. *Journal of Colloid and Interface Science*, 98(1), 290-291.

Ding, A., Nie, W., Huang, X., Chi, X., Sun, J., Kerminen, V.-M., & Yang, X. (2016). Long-term observation of air pollution-weather/climate interactions at the SORPES station: a review and outlook. *Frontiers of Environmental Science & Engineering*, 10(5), 1-15.

Bajjali, W. (2017). *ArcGIS for environmental and water issues*: Springer.

Frenken, K. (2009). Irrigation in the Middle East region in figures AQUASTAT Survey-2008. *Water Reports* (34).

Fu, C., Ding, A., & Wu, J. (2017). Review on studies of air pollution and climate change interactions in Monsoon Asia. *The Global monsoon system: Research and forecast*, 315-326.

Gakidou, E., Afshin, A., Abajobir, A.A., Abate, K.H., Abbafati, C., Abbas, K.M., …, & Aboyans, V. (2017). Global, regional, and national comparative risk assessment of 84 behavioural, environmental and occupational, and metabolic risks or clusters of risks, 1990–2016: a systematic analysis for the Global Burden of Disease Study 2016. *The Lancet*, 390(10100), 1345-1422.

Garnero, G., & Godone, D. (2013). Comparisons between different interpolation techniques. *The International Archives of the Photogrammetry, Remote Sensing and*

Spatial Information Sciences, 5, W3.

Gorai, A.K., Tchounwou, P.B., Biswal, S., & Tuluri, F. (2018). Spatio-temporal variation of particulate matter (PM2. 5) concentrations and its health impacts in a mega city, Delhi in India. *Environmental health insights,* 12, 1178630218792861.

Husar, R.B., Husar, J.D., & Martin, L. (2000). Distribution of continental surface aerosol extinction based on visual range data. *Atmospheric Environment,* 34(29-30), 5067-5078.

Hassan, S.F. (2018). *Modeling Infrastructure Maintenance Contracts in a Geospatial Database.*

Hessl, A., Miller, J., Kernan, J., Keenum, D., & McKenzie, D. (2007). Mapping paleo-fire boundaries from binary point data: comparing interpolation methods. *The Professional Geographer,* 59(1), 87-104.

Huang, F., Liu, D., Tan, X., Wang, J., Chen, Y., & He, B. (2011). Explorations of the implementation of a parallel IDW interpolation algorithm in a Linux cluster-based parallel GIS. *Computers & Geosciences,* 37(4), 426-434.

Jassim, S.Z., & Goff, J.C. (2006). *Geology of Iraq*: DOLIN, sro, distributed by Geological Society of London.

Kampa, M., & Castanas, E. (2008). Human health effects of air pollution. *Environmental pollution,* 151(2), 362-367.

Kiai, C., Kanali, C., Sang, J., & Gatari, M. (2021). Spatial Extent and Distribution of Ambient Airborne Particulate Matter ($PM_{2.5}$) in Selected Land Use Sites in Nairobi, Kenya. *Journal of Environmental and Public Health*.

Li, J., Han, X., Jin, M., Zhang, X., & Wang, S. (2019). Globally analyzing spatiotemporal trends of anthropogenic $PM_{2.5}$ concentration and population's PM2. 5 exposure from 1998 to 2016. *Environment international,* 128, 46-62.

World Health Organization (2006). *Air quality guidelines: global update 2005: particulate matter, ozone, nitrogen dioxide, and sulfur dioxide*: World Health Organization.

Pöschl, U. (2005). Atmospheric aerosols: composition, transformation, climate and health effects. *Angewandte Chemie International Edition,* 44(46), 7520-7540.

Pope III, C.A., Burnett, R.T., Turner, M.C., Cohen, A., Krewski, D., Jerrett, M., Gapstur, S.M., & Thun, M.J. (2011). Lung cancer and cardiovascular disease mortality associated with ambient air pollution and cigarette smoke: shape of the exposure–response relationships. *Environmental Health Perspectives,* 119(11), 1616-1621.

Reimann, C., Filzmoser, P., Garrett, R., & Dutter, R. (2011). *Statistical Data Analysis Explained: Applied Environmental Statistics with R*: John Wiley & Sons.

Robinson, T., & Metternicht, G. (2003). A comparison of inverse distance weighting and ordinary kriging for characterising within-paddock spatial variability of soil properties in Western Australia. *Cartography*, 32(1), 11-24.

Sánka, O. (2015). *Use of Geographic Information System in Environmental Science.* PhD thesis, Masarykova univerzita, Prırodovedecká fakulta.

Thurston, G.D., Burnett, R.T., Turner, M.C., Shi, Y., Krewski, D., Lall, R. & Diver, W.R. (2016). Ischemic heart disease mortality and long-term exposure to source-related components of US fine particle air pollution. *Environmental Health Perspectives*, 124(6), 785-794.

Wang, J., Xie, X., & Fang, C. (2019). Temporal and spatial distribution characteristics of atmospheric particulate matter (PM_{10} and $PM_{2.5}$) in Changchun and analysis of its influencing factors. *Atmosphere,* 10(11), 651.

Wark, K., & Warner, C.F. (1981). Air pollution: its origin and control.

Welburn, A. (1988). *Air Pollution and Acid Rain: the Biological Impact*: Longman Scientific & Technical.

Wid, M.S., Yaseen K.A. & Al-Jiboori M.H. (2022). Correlation coefficient analysis between PM2.5 concentrations and some meteorological parameters in Iraq, accepted by *Iraqi Journal of Agriculture,* 55(4).

Zubkova, G. (2003). *Analysis of Ambient Fine Particulate Matter, $PM_{2.5}$, in Pittsburgh Using Time-Series Techniques and Meteorology.* Ohio University.